August

[Article]

含 CL-20 的改性双基推进剂的热行为及非等温反应动力学

徐司雨　　　赵凤起 *　　　仪建华　　　胡荣祖　　　高红旭

李上文　　　郝海霞　　　裴　庆

(西安近代化学研究所, 西安　710065)

摘要：　用 DSC 和 TG 方法研究了含六硝基六氮杂异伍兹烷(CL-20)的改性双基推进剂在常压(0.1 MPa)和高压(4 和 7 MPa)下的热行为和高压下的热分解反应动力学. 结果表明, 该推进剂常压下 DSC 曲线有 3 个放热峰, 相应 TG 曲线有 3 个失重过程; 而高压下 DSC 曲线只有一个放热峰, 高压下放热峰的峰温随加热速率增大而升高. 高压下该推进剂放热分解反应机理和反应动力学参数受测试环境压强影响较弱, 反应机理是随机成核和随后生长, 放热分解反应的动力学方程可以表示为, 4 MPa 时, $d\alpha/dt=10^{14.5}(1-\alpha)[-\ln(1-\alpha)]^{1/3}e^{-17981.7/T}$; 7 MPa 时, $d\alpha/dt=10^{14.7}(1-\alpha)\cdot[-\ln(1-\alpha)]^{1/3}e^{-18138.1/T}$.

关键词：　推进剂；　热重分析；　差示扫描量热分析；　非等温反应动力学；　CL-20
中图分类号：　O643

Thermal Behavior and Non-Isothermal Decomposition Reaction Kinetics of Composite Modified Double Base Propellant Containing CL-20

XU Si-Yu　　　ZHAO Feng-Qi *　　　YI Jian-Hua　　　HU Rong-Zu　　　GAO Hong-Xu

LI Shang-Wen　　　HAO Hai-Xia　　　PEI Qing

(*Xi'an Modern Chemistry Research Institute, Xi'an　710065, P. R. China*)

Abstract：　Thermal behavior under pressures of 0.1, 4, and 7 MPa and non-isothermal decomposition reaction kinetics under pressures of 4 and 7 MPa of the composite modified double base propellant containing hexanitrohexaazaisowurtzitane (CL-20-CMDB propellant) were investigated by differential scanning calarimetry (DSC) and thermogravimetry (TG). The results showed that there were three exothermic peaks on DSC curve and three mass loss stages on TG curve under 0.1 MPa. There was only one exothermic peak on the DSC curve under 4 and 7 MPa. The exothermic peak temperatures under 4 and 7 MPa increased with increasing the heating rate. The exothermic decomposition reaction mechanism and kinetic parameters of the propellant changed little with testing surroundings. The reaction mechanism was random nucleation and then growth. The kinetic equations of exothermical decomposition reaction can be expressed as, $d\alpha/dt=10^{14.5}(1-\alpha)[-\ln(1-\alpha)]^{1/3}e^{-17981.7/T}$ (under 4 MPa) and $d\alpha/dt=10^{14.7}(1-\alpha)[-\ln(1-\alpha)]^{1/3}e^{-18138.1/T}$ (under 7 MPa).

Key Words：　Propellant；　Thermogravimetric analysis；　Differential scanning calarimetry；　Non-isothermal reaction kinetics；　CL-20

Hexanitrohexaazaisowurtzitane（CL-20）is an ecologically safe, high-energy density material with a cage structure. Compared to other nitramines, such as hexogen（RDX）and octogen (HMX), CL-20 has six N—NO₂ groups in its polycyclic structure （RDX and HMX have three and four N—NO₂ groups, respectively), resulting in an increase in both density and heat of formation. So CL-20 can increase the specific impulse and density of solid propellant greatly. Today, it is considered as the most powerful explosive and has great applying value in solid propellant field. In the view of its superior performance, CL-20 can be regarded as a deputy of the next generation propellant raw material replacing various energetic compounds like RDX

and HMX[1]. Now, there are some reports on the synthesis, polymorphism, spectroscopy, combustion characteristics, and thermal behavior of CL-20[2–15]. CL-20 displays a multistep decomposition process at various heating rates. The residue of CL-20 remaining after many hours at 478.2 K is about 17% of the original sample mass and is stable up to at least 973.2 K[10]. Thermal decomposition of CL-20 has been determined to follow an auto catalytic behavior[15]. However, the thermal decomposition reaction kinetics of composite modified double base propellant containing CL-20 (CL-20-CMDB propellant) has not been reported. In this article, the decomposition reaction kinetics of non-catalyzed CL-20-CMDB propellant has been investigated by non-isothermal method under 4 and 7 MPa pressures and static nitrogen gas conditions. The mass loss stages of CL-20-CMDB propellant have been studied, too.

1 Experimental

1.1 Sample

The sample used in the experiments is CL-20-CMDB propellant, whose composition in mass fraction is 64.7% of nitrocellulose and nitroglycerin, 28% of CL-20 and 7.3% of stabilizer and processing adjuvant.

1.2 Equipment and conditions

DSC experiments were carried out on a differential scanning calorimeter (Model DSC910S, TA Co., USA). The accuracies of temperature and heat flow are 0.1 K and 1 W·g⁻¹, respectively. Samples with mass less than 2.00 mg were heated at heating rates (β) of 5, 10, 20, and 25 K·min⁻¹. Pressure was obtained by filling nitrogen gas (purity, 99.999%) in the heating furnace. Thermogravimetric (TG) analyses of CL-20-CMBD propellant samples were carried out on a thermogravimetric analyzer (Model TGA2950, TA Co., USA). The accuracies of temperature and mass are 0.1 K and 1%, respectively. Samples under atmospheric pressure were heated with a heating rate of 10 K·min⁻¹ and a nitrogen gas flow of 40 mL·min⁻¹.

2 Results and discussion

2.1 Thermal decomposition behaviors of CL-20-CMDB propellant

The DSC curves at different heating rates and TG-DTG curves at a heating rate of 10 K·min⁻¹ under 0.1 MPa for CL-20-CMDB propellant sample are shown in Figs.1 and 2, respectively. There are three exothermic peaks on every DSC curve at different heating rates under 0.1 MPa. With the increase of heating rate, the peak temperature of every exothermic decomposition of propellant shifted towards higher temperature. There are three mass loss stages (stages I, II, and III) in TG curve, corresponding to the three peaks in DTG curve. Stage I begins at 336.9 K and ends at 447.6 K, with a summit peak at 415.7 K in DTG curve, accompanied with 29% mass loss. It is mainly attributed to the volatilization and decomposition of nitroglycerine (NG). Stage II begins at 447.6 K and ends at 504.6 K, with a summit peak at 483.7 K in DTG curve, accompanied with 36% mass loss. It is
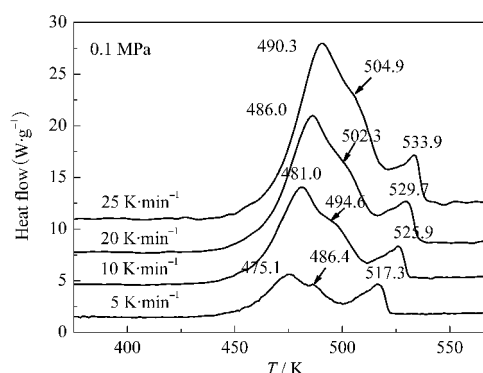

Fig.1 DSC curves for sample at different heating rates under 0.1 MPa

mainly attributed to the decomposition of nitrocellulose (NC), corresponding to the obvious peak in DSC curve in the temperature range. Stage II is caused by the main exothermic decomposition reaction. Stage III begins at 504.6 K and ends at 530.5 K, with a summit peak at 517.9 K in DTG curve, accompanied with 17% mass loss. It is mainly attributed to the part decomposition of the CL-20, corresponding to the obvious peak in DSC curve in the temperature range. There are a few remains at the end of decomposition.

The DSC curves at different heating rates under 4 and 7 MPa for CL-20-CMDB propellant sample are shown in Fig.3. There is only an exothermic peak on the DSC curve under 4 and 7 MPa, which appears very different with that under 0.1 MPa. It indicates that pressure influences thermal decomposition process greatly, and concentrates the exothermic district of the propellant sample. With the increase of heating rate, the onset temperature, peak temperature, and final temperature of the exothermic decomposition of propellant shift towards higher temperature. The exothermic peak temperature at same heating rate decreases with pressure increasing.

2.2 Non-isothermal reaction kinetics

In order to study the thermal decomposition mechanism of the main exothermic reaction stage (main exothermic peak) under propellant working pressure and obtain the corresponding kinetic parameters (apparent activation energy (E_a), pre-exponential
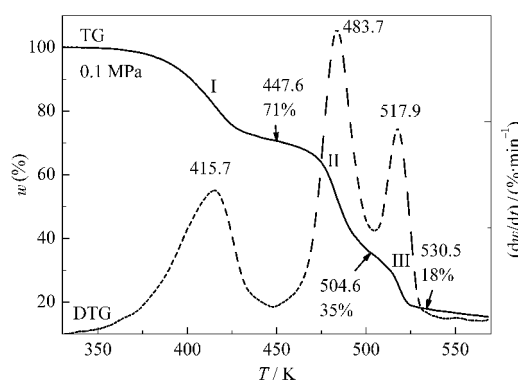

Fig.2 TG-DTG curves for sample at a heating rate of 10 K·min⁻¹ under 0.1 MPa
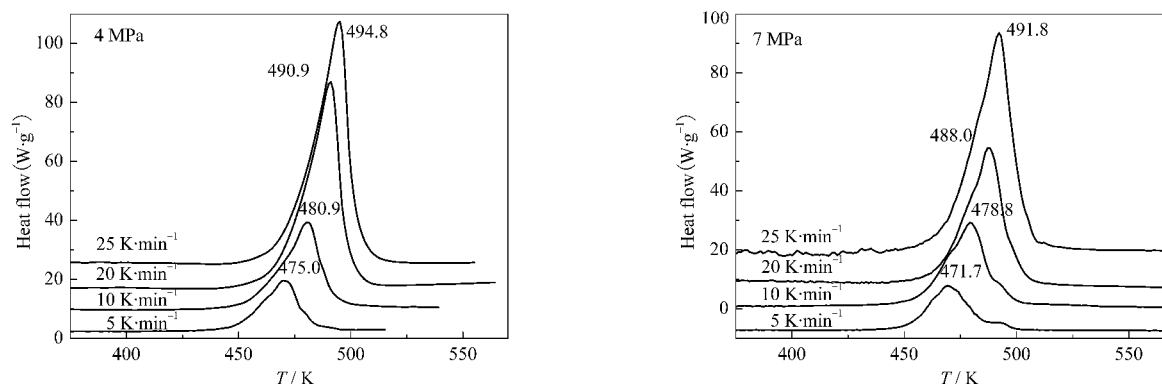
Fig.3   DSC curves for sample at different heating rates under 4 and 7 MPa

Table 1   Kinetic analysis methods

Method	Equation		
Ordinary-integral	$\ln[G(\alpha)/T^2]=\ln[(AR/\beta E_a)(1-2RT/E_a)]-E_a/RT$		(1)
MacCallum-Tanner	$\lg[G(\alpha)]=\lg(AE_a/\beta R)-0.4828E_a^{0.4357}-(0.449+0.217E_a)/(0.001T)$	(E_a in 4.184 kJ·mol^{-1})	(2)
Šatava-Šesták	$\lg[G(\alpha)]=\lg(AE_a/\beta R)-2.315-0.4567E_a/RT$		(3)
Agrawal	$\ln[G(\alpha)/T^2]=\ln\{(AR/\beta E_a)[(1-2(RT/E_a)]/[1-5(RT/E_a)^2]\}-E_a/RT$		(4)
Flynn-Wall-Ozawa	$\ln\beta=\lg\{AE_a/[RG(\alpha)]\}-2.315-0.4567E_a/RT$		(5)
Kissinger	$\ln(\beta_i/T_{pi}^2)=\ln(AR/E_a)-E_a/RT_{pi}$ $(i=1, 2, 3, \cdots)$		(6)

constant (A)) and the most probable kinetic model function, the DSC curves at heating rates of 5, 10, 20, and 25 K·min^{-1} were dealt by mathematic means, and five integral methods [Eqs.(1)–(5)] and one differential methods [Eq.(6)] listed in Table 1 were employed[16,17]. Where α is the conversion degree of sample reacted; T is the temperature (K) at time of t; R is the gas constant; $f(\alpha)$ and $G(\alpha)$ are the differential model function and the integral model function, respectively, and the meanings of E_a, A, β, and T_p are the same as mentioned before. The data needed for the equations of the integral and differential methods, i, α_i, β, T_i, T_p, (dα/dT)$_i$ ($i=1, 2, 3, \cdots$) were obtained from the DSC curves and summarized in Table 2.

The values of E_α obtained by Ozawa′s method [Eq.(5)] with α changing from 0.01 to 1.00 are shown in Table 3. From Fig.4, we can see that activation energies change little with the increase of conversion degree. In the range of 0.01–0.85(α) under 4 MPa and 0.10–0.80 (α) under 7 MPa, activation energies change even faintly, which means that the decomposition mechanism of

the processes does not transfer in essence or the transference could be ignored. So, it is feasible to study the reaction mechanism and kinetics in these ranges.

Forty-one types of kinetic model functions in Ref.[15] and the original data tabulated in Table 2 were put into Eqs.(1)–(6) for calculations, respectively. The values of E_a, $\lg A$, linear correlation coefficient (r), and standard mean square deviation (Q) under 4 and 7 MPa can be calculated on the computer with the linear least squares method at various heating rates of 5, 10, 20, and 25 K·min^{-1}. The most probable mechanism function was selected by the better values of r, and Q based on the following four conditions: (1) the values of E_a and $\lg A$ selected were in the ordinary range of the thermal decomposition kinetic parameters for solid materials [E_a/(kJ·mol^{-1})=80–250 and $\lg(A/s^{-1})$=7–30]; (2) linear correlation coefficient (r) was greater than 0.98; (3) the values of E_a and $\lg A$ obtained with the differential and integral methods were approximately the same; (4) the mechanism function selected must be in agreement with the tested sample state.
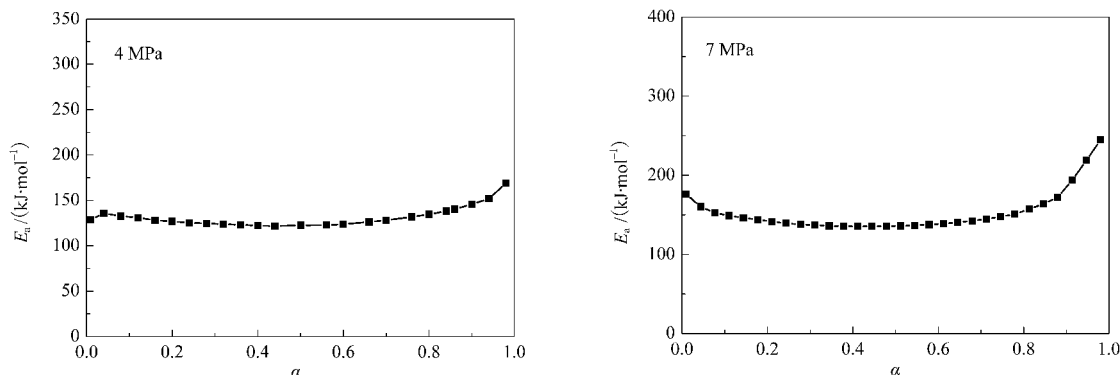

Fig.4 E_a *vs* α curves obtained by Ozawa′s method under 4 and 7 MPa

Table 2   Data for decomposition processes of sample at different heating rates from DSC curves

α	T/K (under 4 MPa)				T/K (under 7 MPa)			
	β/(K·min⁻¹)				β/(K·min⁻¹)			
	5	10	20	25	5	10	20	25
0.01	440.0	446.2	456.3	459.8	440.9	449.1	452.8	455.8
0.02	444.5	451.0	460.9	464.2	445.0	453.4	457.3	461.0
0.03	447.4	453.9	463.8	467.0	447.5	456.0	460.1	464.2
0.04	449.3	456.0	466.0	469.0	449.2	457.8	462.1	466.6
0.05	450.8	457.6	467.6	470.7	450.6	459.2	463.6	468.4
0.06	451.9	458.9	469.0	472.0	451.7	460.3	464.9	469.9
0.07	452.9	460.0	470.2	473.2	452.6	461.4	466.0	471.2
0.08	453.8	461.0	471.3	474.3	453.4	462.3	466.9	472.3
0.09	454.6	461.9	472.2	475.2	454.2	463.1	467.8	473.2
0.10	455.3	462.7	473.0	476.1	454.8	463.8	468.6	474.1
0.11	456.0	463.4	473.8	476.9	455.4	464.5	469.3	474.9
0.12	456.6	464.1	474.6	477.7	456.0	465.1	469.9	475.6
0.13	457.2	464.8	475.2	478.4	456.5	465.7	470.6	476.3
0.14	457.8	465.4	475.9	479.1	457.0	466.2	471.1	476.9
0.15	458.3	466.0	476.5	479.7	457.5	466.7	471.7	477.5
0.16	458.8	466.6	477.1	480.4	457.9	467.2	472.2	478.1
0.17	459.2	467.2	477.7	480.9	458.3	467.7	472.7	478.6
0.18	459.7	467.7	478.2	481.5	458.7	468.1	473.1	479.1
0.19	460.1	468.2	478.7	482.1	459.0	468.5	473.6	479.6
0.20	460.5	468.7	479.2	482.6	459.3	468.9	474.0	480.1
0.21	460.9	469.2	479.7	483.1	459.7	469.3	474.4	480.6
0.22	461.2	469.6	480.1	483.6	460.0	469.7	474.8	481.0
0.23	461.6	470.1	480.6	484.1	460.3	470.1	475.2	481.4
0.24	462.0	470.5	481.0	484.5	460.5	470.4	475.5	481.8
0.25	462.3	470.9	481.5	485.0	460.8	470.8	475.9	482.2
0.26	462.7	471.3	481.9	485.4	461.1	471.1	476.3	482.6
0.27	463.0	471.7	482.3	485.9	461.4	471.5	476.6	483.0
0.28	463.3	472.1	482.6	486.3	461.7	471.8	476.9	483.4
0.29	463.6	472.5	483.0	486.7	461.9	472.1	477.3	483.7
0.30	464.0	472.9	483.4	487.1	462.2	472.5	477.6	484.1
0.31	464.3	473.2	483.8	487.5	462.5	472.8	477.9	484.4
0.32	464.6	473.6	484.1	487.8	462.7	473.1	478.2	484.7
0.33	464.9	474.0	484.5	488.2	463.0	473.4	478.5	485.1
0.34	465.2	474.3	484.8	488.6	463.3	473.7	478.8	485.4
0.35	465.4	474.6	485.2	489.0	463.5	474.0	479.1	485.7
0.36	465.7	475	485.5	489.3	463.8	474.3	479.4	486.0
0.37	466.0	475.3	485.8	489.7	464.1	474.5	479.7	486.3
0.38	466.3	475.6	486.1	490.0	464.3	474.8	480.0	486.6
0.39	466.5	475.9	486.5	490.4	464.6	475.1	480.3	487.0
0.40	466.8	476.3	486.8	490.7	464.8	475.4	480.6	487.2
0.41	467.1	476.6	487.1	491.0	465.1	475.7	480.8	487.5
0.42	467.3	476.9	487.4	491.3	465.4	475.9	481.1	487.8
0.43	467.6	477.2	487.7	491.7	465.6	476.2	481.4	488.1
0.44	467.8	477.5	488.0	492.0	465.9	476.5	481.6	488.4
0.45	468.1	477.7	488.3	492.3	466.1	476.8	481.9	488.6
0.46	468.3	478	488.6	492.6	466.4	477.0	482.2	488.9
0.47	468.5	478.3	488.8	492.9	466.6	477.3	482.4	489.2
0.48	468.7	478.5	489.1	493.1	466.9	477.5	482.6	489.4
0.49	469.0	478.8	489.4	493.4	467.1	477.8	482.9	489.7

Continued Table 2

	T/K (under 4 MPa)				T/K (under 7 MPa)			
α	$\beta/(K \cdot min^{-1})$				$\beta/(K \cdot min^{-1})$			
	5	10	20	25	5	10	20	25
0.50	469.2	479.1	489.6	493.7	467.4	478.0	483.1	490.0
0.51	469.4	479.3	489.8	493.9	467.6	478.3	483.3	490.2
0.52	469.6	479.5	490.1	494.2	467.9	478.5	483.5	490.4
0.53	469.8	479.8	490.3	494.4	468.1	478.7	483.7	490.7
0.54	470.0	480	490.5	494.6	468.3	479.0	484.0	490.9
0.55	470.2	480.2	490.7	494.8	468.6	479.2	484.2	491.1
0.56	470.4	480.4	490.9	495.0	468.8	479.4	484.4	491.3
0.57	470.6	480.6	491.1	495.2	469.1	479.6	484.6	491.6
0.58	470.8	480.9	491.3	495.4	469.3	479.9	484.8	491.8
0.59	471.0	481.1	491.5	495.6	469.5	480.1	485.0	492.0
0.60	471.2	481.3	491.6	495.7	469.8	480.3	485.2	492.2
0.61	471.4	481.5	491.8	495.9	470.0	480.5	485.4	492.4
0.62	471.6	481.7	491.9	496.0	470.3	480.7	485.6	492.6
0.63	471.8	481.9	492.1	496.2	470.5	480.9	485.8	492.8
0.64	472.0	482.1	492.2	496.3	470.8	481.1	486.0	493.0
0.65	472.2	482.3	492.4	496.4	471.1	481.3	486.2	493.2
0.66	472.4	482.5	492.5	496.6	471.3	481.5	486.4	493.4
0.67	472.6	482.7	492.7	496.7	471.6	481.8	486.6	493.6
0.68	472.8	482.8	492.8	496.8	471.8	482.0	486.8	493.8
0.69	473.0	483.0	492.9	497.0	472.1	482.2	487.0	494.0
0.70	473.2	483.2	493.1	497.1	472.4	482.4	487.2	494.2
0.71	473.4	483.4	493.2	497.2	472.6	482.7	487.4	494.4
0.72	473.6	483.6	493.3	497.3	472.9	482.9	487.6	494.6
0.73	473.8	483.8	493.4	497.4	473.2	483.1	487.8	494.8
0.74	474.0	484.0	493.6	497.6	473.5	483.4	488.0	495.0
0.75	474.2	484.2	493.7	497.7	473.9	483.6	488.2	495.2
0.76	474.4	484.4	493.8	497.8	474.2	483.8	488.4	495.4
0.77	474.7	484.6	494.0	497.9	474.5	484.1	488.6	495.6
0.78	474.9	484.8	494.1	498.1	474.9	484.4	488.9	495.8
0.79	475.1	485.1	494.3	498.2	475.3	484.6	489.1	496.1
0.80	475.4	485.3	494.4	498.3	475.8	484.9	489.4	496.3
0.81	475.6	485.6	494.6	498.5	476.2	485.2	489.6	496.6
0.82	475.9	485.9	494.7	498.6	476.7	485.5	489.9	496.8
0.83	476.1	486.2	494.9	498.8	477.2	485.9	490.1	497.1
0.84	476.4	486.5	495.0	499.0	477.7	486.3	490.4	497.4
0.85	476.8	486.8	495.2	499.2	478.3	486.6	490.7	497.7
0.86	477.1	487.2	495.4	499.4	478.9	487.0	491.1	498.0
0.87	477.5	487.6	495.6	499.6	479.5	487.5	491.4	498.3
0.88	477.9	488.0	495.9	499.9	480.0	488.0	491.8	498.6
0.89	478.4	488.4	496.2	500.2	481.0	488.5	492.2	499.0
0.90	478.9	488.8	496.5	500.6	481.9	489.2	492.7	499.4
0.91	479.4	489.3	496.8	500.9	482.9	489.8	493.2	499.8
0.92	479.9	489.9	497.2	501.4	484.0	490.5	493.8	500.3
0.93	480.5	490.6	497.7	501.9	485.3	491.3	494.4	500.8
0.94	481.1	491.5	498.3	502.5	486.5	492.1	495.1	501.4
0.95	482.0	492.7	498.9	503.2	487.9	492.9	495.9	502.1
0.96	483.0	494.1	499.7	504.1	489.2	493.8	496.7	502.9
0.97	484.4	496.1	500.7	505.3	490.5	494.9	497.7	503.9
0.98	486.5	499.1	502.1	506.9	492.0	496.3	499.1	505.2
0.99	489.4	504.9	504.3	509.9	494.0	498.4	501.2	507.1
1.00	495.4	521.9	515.8	526.2	506.0	506.0	509.7	517.7
	T_p=475.0 K	T_p=480.9 K	T_p=490.9 K	T_p=494.8 K	T_p=471.7 K	T_p=478.8 K	T_p=488.0 K	T_p=491.8 K

Table 3   Kinetic parameters for the decomposition process of sample under 4 and 7 MPa

Method	$\beta/(K \cdot min^{-1})$	4 MPa				7 MPa			
		$E_a/(kJ \cdot mol^{-1})$	$lg(A/s^{-1})$	r	Q	$E_a/(kJ \cdot mol^{-1})$	$lg(A/s^{-1})$	r	Q
Ordinary-integral	5	156.6	15.2	0.9998	0.0225	148.2	14.3	0.9949	0.1543
	10	142.0	13.5	0.9992	0.0789	149.9	14.4	0.9997	0.0124
	20	151.2	14.5	0.9971	0.2701	155.9	15.2	0.9998	0.0091
	25	147.8	14.1	0.9963	0.3715	148.8	14.3	0.9993	0.0225
MacCallum-Tanner	5	156.8	15.2	0.9999	0.0040	148.4	14.2	0.9962	0.0289
	10	142.2	13.5	0.9992	0.0143	150.2	14.4	0.9996	0.0022
	20	151.7	14.5	0.9972	0.0509	156.4	15.2	0.9997	0.0017
	25	148.3	14.1	0.9971	0.0700	149.4	14.3	0.9994	0.0042
Šatava-Šesták	5	156.3	15.2	0.9998	0.0040	148.3	14.3	0.9955	0.0286
	10	142.5	13.5	0.9991	0.0146	150.0	14.4	0.9996	0.0021
	20	151.4	14.5	0.9973	0.0507	155.9	15.2	0.9997	0.0016
	25	148.1	14.1	0.9960	0.0701	149.3	14.3	0.9994	0.0043
Agrawal	5	156.6	15.2	0.9997	0.0225	148.2	14.3	0.9950	0.1542
	10	142.0	13.5	0.9990	0.0785	149.9	14.4	0.9996	0.0122
	20	151.2	14.5	0.9969	0.2701	155.9	15.2	0.9997	0.0091
	25	147.8	14.1	0.9957	0.3715	148.9	14.3	0.9994	0.0227
Mean		149.5	14.3			150.8	14.5		
Flynn-Wall-Ozawa		147.8		0.9918		146.7		0.9972	
Kissinger		147.4	15.8	0.9908		146.3	15.8	0.9969	

The results satisfying the conditions mentioned above are listed in Tables 3.

The values of E_a and lgA obtained from a single non-isothermal DSC curve are in good agreement approximately with the values calculated by Kissinger′s method and Ozawa′s method. Therefore, we conclude that the reaction mechanisms of the main exothermal decomposition processes of the sample under 4 and 7 MPa are the same one. It is classified as random nucleation and then growth, and the mechanism function is the Avramic Erofeev Equation with $n=2/3$, and $G(\alpha)=[-\ln(1-\alpha)]^{2/3}$, $f(\alpha)=(3/2)(1-\alpha)[-\ln(1-\alpha)]^{1/3}$. Substituting $f(\alpha)$ with $(3/2)(1-\alpha)[-\ln(1-\alpha)]^{1/3}$, $E_a/(kJ \cdot mol^{-1})$ with 149.5 and lg (A/s^{-1}) with 14.3 into Eq.(7)

$$d\alpha/dt = Af(\alpha)e^{-E/RT} \qquad (7)$$

the kinetic equation of exothermal decomposition reaction under 4 MPa may be described as

$$d\alpha/dt = 10^{14.5}(1-\alpha)[-\ln(1-\alpha)]^{1/3}e^{-17981.7/T}$$

Substituting $f(\alpha)$ with $(3/2)(1-\alpha)[-\ln(1-\alpha)]^{1/3}$, $E_a/(kJ \cdot mol^{-1})$ with 150.8 and $lg(A/s^{-1})$ with 14.5 into Eq.(7), the kinetic equation of exothermal decomposition reaction under 7 MPa may be described as

$$d\alpha/dt = 10^{14.7}(1-\alpha)[-\ln(1-\alpha)]^{1/3}e^{-18138.1/T}$$

3   Conclusions

The decomposition reaction of CL-20-CMDB propellant under 0.1 MPa can be divided into three stages: the volatilization and decomposition of NG, exothermic decomposition of NC, and exothermic decomposition of CL-20. There is only one exothermic decomposition peak of this propellant under pressures of 4 and 7 MPa. The exothermic decomposition reaction mechanisms at 4 and 7 MPa obey random nucleation and then growth rule.

The kinetic parameters of the reaction are: $E_a=149.5$ kJ $\cdot$ mol^{-1}, $A=10^{14.3}$ s^{-1} under 4 MPa and $E_a=150.8$ kJ $\cdot$ mol^{-1}, $A=10^{14.5}$ s^{-1} under 7 MPa. The kinetic equation of exothermic decomposition reaction can be expressed as

$$d\alpha/dt = 10^{14.5}(1-\alpha)[-\ln(1-\alpha)]^{1/3}e^{-17981.7/T} \text{ (under 4 MPa)}$$

and

$$d\alpha/dt = 10^{14.7}(1-\alpha)[-\ln(1-\alpha)]^{1/3}e^{-18138.1/T} \text{ (under 7 MPa)}.$$

References

1   Li, S. W.; Zhao, F. Q.; Wang, Q. L.; Wang, X. F. *Chin. J. Explos. & Propell.*, **1998, 21**(4): 51   [李上文, 赵凤起, 王琼林, 王晓峰. 火炸药学报, **1998, 21**(4): 51]

2   Ou, Y. X.; Xu, Y. J.; Chen, B. R.; Liu, L. H.; Wang, C. *Chin. J. Org. Chem.*, **2000, 20**(4): 556   [欧育湘, 徐永江, 陈博仁, 刘利华, 王 才. 有机化学, **2000, 20**(4): 556]

3   Russell, T. P.; Miller, P. J.; Piermarini, G. J.; Block, S. *J. Phys. Chem.*, **1993, 97**: 1993

4   Ou, Y. X.; Jia, H. P.; Chen, B. R.; Xu, Y. J.; Pan, Z. L.; Chen, J. T.; Zheng, F. P. *Chin. J. Explos. & Propell.*, **1998, 21**(4): 41   [欧育湘, 贾会平, 陈伯仁, 徐永江, 潘则林, 陈江涛, 郑福平. 火炸药学报, **1998, 21**(4): 41]

5   Foltz, M. F.; Coon, C. L.; Garcia, F.; Nichols, A. L. *Propell. Explos. Pyrotech.*, **1994, 19**: 19

6   Foltz, M. F.; Coon, C. L.; Garcia, F.; Nichols, A. L. *Propell. Explos. Pyrotech.*, **1994, 19**: 133

7   Ou, Y. X.; Liu, J. Q.; Chen, B. R. High energetic density materials. Beijing: National Defence Engineering Publisher, 2005, 1   [欧育湘, 刘进全, 陈博仁. 高能量密度化合物. 北京: 国防工业出版社, 2005, 1]

8   Boris, K.; Vadim, N.; Nikita C.; Tatiana, L. Kinetics of thermal decomposition of hexanitrohexaazaisowurtzitane. Germany: Institute

Chemische Technologie. Fraunhofer. In: Proc. of the 30th Int. Annual
Conf. of ICT, Karlsruhe, June 29-July 2, 1999

9   Patil, D. G.; Brill, T. B. *Combust. Flame.*, **1991, 87**: 145

10 Patil, D. G.; Brill, T. B. *Combust. Flame.*, **1993, 92**: 456

11   An, H. M.; Liu, Y. F.; Li, X. M.; Yang, R. J.; Tan, H. M. *Chin. J.
    Explos. & Propell.*, **2001, 24**(1): 36   [安红梅, 刘云飞, 李晓萌,
    杨荣杰, 谭惠民. 火炸药学报, **2001, 24**(1): 36]

12 An, H. M.; Liu, Y. F.; Li, Y. P.; Yang, R. J.; Tan, H. M. *Chin. J.
    Explos. & Propell.*, **2000, 23**(4): 27   [安红梅, 刘云飞, 李玉平,
    杨荣杰, 谭惠民. 火炸药学报, **2000, 23**(4): 27]

13 Liu, S. E.; Zhao, F. Q.; Li, S. W.; Liu, Z. R.; Yin, C. M. *Chin.
    J. Explos. & Propell.*, **1998, 21**(2): 27   [刘所恩, 赵凤起, 李上文,
    刘子如, 阴翠梅. 火炸药学报, **1998, 21**(2): 27]

14 Nedelko, V. V.; Chukanov, N. V.; Raevskii, A. V.; Korsounskii, B.

L.; Larikova, T. S.; Kolesova, O. I. *Propell. Explos. Pyrotech.*,
2000, 25(5): 255

15 Liu, Y. New applications of thermal analysis technique on
    investigation of energetic material decomposition chemistry. Xi'an:
    Xi'an Modern Chemistry Research Institute, 2003: 4   [刘   艳.
    热分析技术在研究含能材料热分解化学中的新应用. 西安: 西安
    近代化学研究所, 2003: 4]

16 Hu, R. Z.; Shi, Q. Z. Thermal analysis kinetics. Beijing: Science
    Press, 2001   [胡荣祖, 史启祯. 热分析动力学. 北京: 科学出版
    社, 2001]

17 Wu, X. M.; Liu, J. H.; Li, W.; Qi, C. S. *Acta Phys. -Chim. Sin.*,
    2006, 22(8): 942   [吴新民, 刘建华, 李   巍, 戚传松. 物理化学
    学报, **2006, 22**(8): 942]